Analysis of FRP-Strengthened RC Beam-Column Joints

Costas P. Antonopoulos[1] and Thanasis C. Triantafillou, M.ASCE[2]

Abstract: Analytical models are presented in this study for the analysis of reinforced concrete joints strengthened with composite materials in the form of externally bonded reinforcement comprising unidirectional strips or flexible fabrics. The models provide equations for stresses and strains at various stages of the response (before or after yielding of the beam or column reinforcement) until the ultimate capacity is reached, defined by concrete crushing or fiber-reinforced polymer (FRP) failure due to fracture or debonding. Solutions to these equations are obtained numerically. The models provide useful information on the shear capacity of FRP-strengthened joints in terms of the quantity and configuration of the externally bonded reinforcement and may be used to design FRP patching for inadequately detailed beam-column joints. A number of case studies are examined in this article, indicating that even low quantities of FRP materials may provide significant enhancement of the shear capacity. The effectiveness of external reinforcement increases considerably if debonding is suppressed and depends heavily on the distribution of layers in the beam and column. The latter depends on the relative quantities of steel reinforcement crossing the joint panel and the level of axial load in the column. Analytical shear strength predictions were in good agreement with test results found in the literature, thus adding confidence to the validity of the proposed models.

DOI: 10.1061/(ASCE)1090-0268(2002)6:1(41)

CE Database keywords: Beam columns; Fiber reinforced materials; Joints; Analytical techniques; Polymers.

Introduction

Reinforced concrete (RC) beam-column joints have been the subject of intensive research over the past few decades. Inadequately detailed joints, especially exterior ones, have been identified as critical structural elements that may fail prematurely due to high shear stresses. Bond failure of longitudinal reinforcement has been observed too, especially in interior joints where rebars are not properly anchored with standard hooks [e.g., Paulay and Priestley (1992)].

Strengthening of RC joints is a rather difficult task. A variety of techniques have been applied to joints, with the most common being the construction of RC or steel jackets [e.g., Alcocer and Jirsa (1993)]. Plain or corrugated steel plates have also been tried [e.g., Beres et al. (1992); Ghobarah et al. (1997)]. To overcome the difficulties and some problems associated with these techniques, namely intensive labor, artful detailing, increased dimensions, corrosion protection, and special attachments, recent research efforts have focused on the use of fiber-reinforced polymers (FRP), which may be epoxy-bonded in the form of flexible sheets or strips with fibers oriented properly so as to carry tension forces due to shear (Fig. 1 is a typical example).

FRP-strengthened joints mainly have been studied experimentally. The results of an extensive test program carried out by the writers on 18 2/3 scale exterior joints are reported in Antonopoulos and Triantafillou (2001). Other studies include those of Pantelides et al. (1997, 1999), who tested two full-scale bridge bents, and Gergely et al. (2000), who tested a series of one-third-scale exterior joints. Shear strengthening of the joints in these studies was achieved in most cases by bonding CFRP sheets in two orthogonal directions. A common conclusion was that even very low quantities of FRP materials (a few layers) increase the shear capacity of RC joints considerably.

Analytical modeling of FRP-strengthened joints has been extremely limited. Gergely et al. (1998) calculated the contribution of the FRP to the shear capacity of a joint by analogy to steel stirrups, assuming that the FRP crossing a potential shear crack in the beam will exhaust its tensile capacity. Tsonos and Stylianidis (1999) followed the same approach but fixed the FRP strain at a value equal to 0.0035. Gergely et al. (2000) repeated this argument and, based on limited test results, fixed the FRP strain to 0.0021, for concrete surfaces prepared with a wire brush, or to 0.0033, for water-jetted concrete surfaces. These approaches are rather oversimplified and, according to the writers' view, fail to capture the real state of stress (and strain) in the joint. Furthermore, fixing the FRP failure strain to a certain value in shear-strengthening applications does not reflect the real behavior [e.g., Triantafillou and Antonopoulos 2000]: depending on its axial stiffness (elastic modulus times thickness), the FRP may debond prematurely at strain levels well below the fracture strain.

Analytical modeling of RC joints (without FRP) has been extensive, and a thorough survey of the relevant literature falls outside the scope of the present study. One of the most powerful models is that of Pantazopoulou and Bonacci (1992), which uses stress equilibrium and strain compatibility to yield the shear strength of a joint with known geometry and reinforcement quantities. In this study, the writers have extended the aforementioned model to account for the effect of externally bonded FRP. They have also developed two computer programs that may be used to trace the state of stress and strain in RC joints strengthened with either unidirectional strips or flexible sheets (the latter may be combined

[1]Graduate Research Assistant, Dept. of Civil Engineering, Univ. of Patras, Patras 26500, Greece.

[2]Associate Professor, Dept. of Civil Engineering, Univ. of Patras, Patras 26500, Greece. E-mail: ttriant@upatras.gr

Note. Discussion open until July 1, 2002. Separate discussions must be submitted for individual papers. To extend the closing date by one month, a written request must be filed with the ASCE Managing Editor. The manuscript for this paper was submitted for review and possible publication on January 9, 2000; revised April 9, 2001. This paper is part of the ***Journal of Composites for Construction***, Vol. 6, No. 1, February 1, 2002. ©ASCE, ISSN 1090-0268/2002/1-41–51/$8.00+$.50 per page.

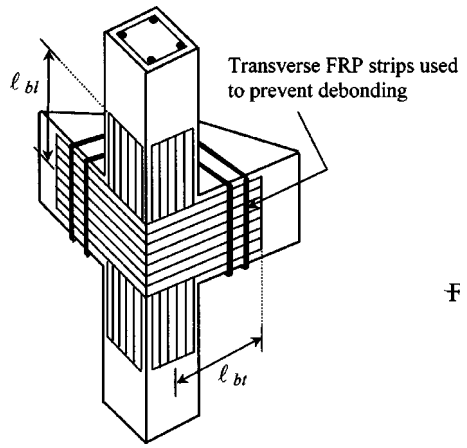

Fig. 1. Schematic illustration of RC joint strengthened with FRP

to form laminates). Following the analytical and numerical formulations, a series of case studies is analyzed and the analytical model compared with existing test results.

Mechanics of RC Joints Strengthened with FRP Strips

Basic Assumptions

A typical beam-column joint is illustrated in Fig. 2. The joint is idealized as a 3D element with dimensions d (width of column), b (width of beam), and h (height of beam). Average stresses in the joint are shown in Fig. 3(a,b). Shear stresses are introduced by direct member action and by bond that develops between the main reinforcement and the joint core concrete. For simplicity, it is assumed that the shear stress, ν, is uniformly distributed over the boundaries of the joint. Furthermore, it is assumed that at the moment of strengthening the joint is already loaded, so that a set of initial normal strains, ϵ_{0t} and ϵ_{0l} in the transverse (beam) and longitudinal (column) direction, respectively, and an initial shear strain, γ_0, have developed.

The principal strains, ϵ_1 and ϵ_2, are related to those in the longitudinal and transverse directions, ϵ_l and ϵ_t, through the following expression:

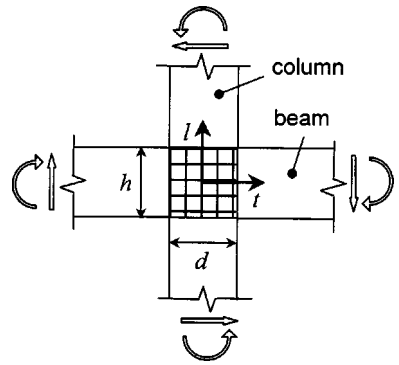

Fig. 2. Moment and shear acting at joint and definition of coordinate system

$$\tan^2\theta = \frac{\epsilon_1 - \epsilon_t}{\epsilon_1 - \epsilon_l} = \frac{\epsilon_2 - \epsilon_l}{\epsilon_2 - \epsilon_t} \tag{1}$$

where θ is the inclination (from the t-axis) of the maximum principal strain ϵ_1. Moreover, assuming that (1) the maximum principal stress in the concrete, σ_1, cannot exceed the tensile capacity, which is taken to be zero; and (2) the directions of principal strains and stresses coincide (this is nearly correct if the reinforcement has not yielded), one may show that

$$\sigma_t = -\nu \tan\theta \tag{2}$$

$$\sigma_l = -\frac{\nu}{\tan\theta} \tag{3}$$

where σ_t and σ_l are the average compressive stress in the concrete in the transverse (t) and longitudinal (l) directions, respectively. Finally, with $\sigma_1 = 0$, the "stress invariant" condition states give the minimum principal stress in the concrete:

$$\sigma_2 = \sigma_t + \sigma_l \tag{4}$$

We would like to note here that the above equations have been derived and used in the work of Pantazopoulou and Bonacci (1992).

Equilibrium Considerations

A key assumption in this section is that strengthening of the joint is carried out through the use of unidirectional strips placed in

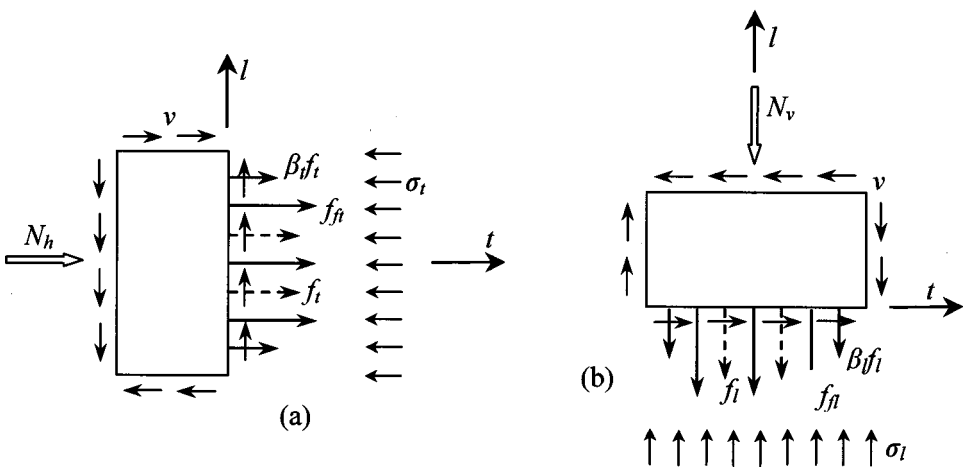

Fig. 3. Stress equilibrium: (a) horizontal forces; (b) vertical forces

two orthogonal directions (vertically and horizontally). Horizontal force equilibrium requires that σ_t satisfy the following relationship:

$$\sigma_t = -(\rho_s + \beta_t \rho_b) f_t - \rho_{ft} f_{ft} - \frac{N_h}{bh} \tag{5}$$

where f_t = average stress in the horizontal stirrups (at midwidth of the joint); ρ_s = stirrup reinforcement ratio; ρ_b = total main beam reinforcement ratio; β_t = factor with values between 0 and 1, relating the magnitude of stresses (or strains) in the main beam reinforcement to the average stirrup stresses (or strains) at the column centerline; f_{ft} = average normal stress in the FRP in the transverse direction (at midwidth of the joint); ρ_{ft} = FRP reinforcement ratio in the transverse direction; and N_h = compressive axial force of the beam (if any). The factor β_t accounts for the bond conditions along the main beam reinforcement: for perfect bond, $\beta_t = 0$; for negligible bond, $\beta_t = 1$ (Pantazopoulou and Bonacci 1992).

Similarly, vertical force equilibrium gives the average longitudinal compressive stress in the concrete, σ_l, as follows:

$$\sigma_l = -(\rho_{c,in} + \beta_l \rho_c) f_l - \rho_{fl} f_{fl} - \frac{N_v}{bd} \tag{6}$$

where f_l = average stress of longitudinal reinforcement of the column inside the joint core at the midheight of the joint; ρ_c = total main column reinforcement ratio (at the boundaries of the joint core); $\rho_{c,in}$ = column reinforcement ratio inside the joint core; β_l = factor that relates the magnitude of stresses (or strains) in the column reinforcement outside the core to the average stresses (or strains) of the reinforcement inside the core at the beam centerline; f_{fl} = average normal stress in the FRP in the longitudinal direction (at midheight of the joint); ρ_{fl} = FRP reinforcement ratio in the longitudinal direction; and N_v = compressive axial force of the column. As above, the factor β_l accounts for the bond conditions along the main column reinforcement (at the boundaries of the core).

To limit the number of variables in the problem, we make the following simplifications: $\rho_t = \rho_s + \beta_t \rho_b$ = effective horizontal reinforcement ratio; $\rho_l = \rho_{c,in} + \beta_l \rho_c$ = effective vertical reinforcement ratio. Moreover, we assume that the effective yield stress of the horizontal reinforcement, f_{yt}, is given as $f_{yt} = (\rho_s f_{sy} + \beta_t \rho_b f_{by})/\rho_t$, where f_{sy} = yield stress of stirrups and f_{by} = yield stress of beam reinforcement. The yield stress of the column reinforcement is denoted as f_{yl}.

Next we analyze all the possible states of joint behavior, namely

Step (a) Before yielding of steel reinforcement;

Step (b) After yielding of effective horizontal reinforcement, before yielding of effective vertical reinforcement;

Step (c) After yielding of both horizontal and vertical reinforcement;

Step (d) After yielding of effective vertical reinforcement, before yielding of effective horizontal reinforcement;

Step (e) Crushing of concrete, defined when the principal compressive stress, σ_2, reaches the crushing strength of concrete. This condition defines failure of the joint and will occur during one of the aforementioned four states; and

Step (f) Failure of the FRP by either debonding or tensile fracture; this may occur before the concrete crushes.

Step (a) Analysis before Yielding of Steel Reinforcement

We start with Eq. (1) and the material constitutive laws:

$$\tan^2\theta = \frac{\epsilon_2 - \epsilon_l}{\epsilon_2 - \epsilon_t} = \left(\frac{\sigma_2}{E_c} - \epsilon_l\right)\left(\frac{\sigma_2}{E_c} - \epsilon_t\right)^{-1} \tag{7}$$

where E_c = is the secant elastic modulus of concrete in the strain under consideration. The stress σ_2 and the strains ϵ_l, ϵ_t are written in terms of ν and $\tan\theta$ using Eqs. (2)–(6), with $f_l = E_s \epsilon_l$, $f_t = E_s \epsilon_t$, $f_{fl} = E_f(\epsilon_l - \epsilon_{0l})$, and $f_{ft} = E_f(\epsilon_t - \epsilon_{0t})$. The elastic modulus of steel is E_s and E_f is the elastic modulus of the FRP in the principal fiber direction. Next, ν is replaced by $-\sigma_t/\tan\theta$, where σ_t is given by Eq. (5). The result is

$$\nu = \frac{1}{\tan\theta}\left[\rho_t E_s \epsilon_t + \rho_{ft} E_f \epsilon_t - \rho_{ft} E_f \epsilon_{0t} + \frac{N_h}{bh}\right] \tag{8}$$

The procedure described above leads to a quadratic polynomial of $\tan^2\theta$:

$$\left\{\frac{1 + \dfrac{1}{n_{sc}(\rho_t + n_{fs}\rho_{ft})}\left[1 - \dfrac{e_h - n_{fc}\rho_{ft}\epsilon_{0t}}{n_{sc}(\rho_t + n_{fs}\rho_{ft})\epsilon_t + e_h - n_{fc}\rho_{ft}\epsilon_{0t}}\right]}{1 + \dfrac{1}{n_{sc}(\rho_l + n_{fs}\rho_{fl})}}\right\} \tan^4\theta$$

$$+ \left\{\frac{e_v - n_{fc}\rho_{fl}\epsilon_{0l}}{[1 + n_{sc}(\rho_l + n_{fs}\rho_{fl})][n_{sc}(\rho_t + n_{fs}\rho_{ft})\epsilon_t + e_h - n_{fc}\rho_{ft}\epsilon_{0t}]}\right\} \tan^2\theta - 1 = 0 \tag{9}$$

where $n_{sc} = E_s/E_c$; $n_{fs} = E_f/E_s$; $e_h = N_h/bhE_c$; and $e_v = N_v/bdE_c$.

Step (b) Analysis after Yielding of Effective Horizontal Reinforcement and before Yielding of Effective Vertical Reinforcement

The analysis is carried out as in Step (a) above with $f_t = f_{yt}$. The shear stress ν is given by Eq. (8), with the product $E_s \epsilon_t$ replaced by f_{yt}, and the polynomial of $\tan\theta$ becomes

$$\left\{\frac{1+\frac{1}{n_{fc}\rho_{ft}}\left[1-\frac{e_h-n_{fc}\rho_{ft}\epsilon_{0t}+n_{sc}\rho_t(f_{yt}/E_s)}{n_{sc}\rho_t(f_{yt}/E_s)+n_{fc}\rho_{ft}\epsilon_t+e_h-n_{fc}\rho_{ft}\epsilon_{0t}}\right]}{1+\frac{1}{n_{sc}(\rho_l+n_{fs}\rho_{fl})}}\right\}\tan^4\theta$$

$$+\left\{\frac{e_v-n_{fc}\rho_{fl}\epsilon_{0l}}{[1+n_{sc}(\rho_l+n_{fs}\rho_{fl})][n_{sc}\rho_t(f_{yt}/E_s)+n_{fc}\rho_{ft}\epsilon_t+e_h-n_{fc}\rho_{ft}\epsilon_{0t}]}\right\}\tan^2\theta-1=0 \tag{10}$$

Step (c). Analysis after Yielding of Both Horizontal and Vertical Reinforcement

The analysis is carried out as in Step (a) above with $f_t=f_{yt}$ and $f_l=f_{yl}$. The shear stress ν is given by Eq. (8) with the product $E_s\epsilon_t$ replaced by f_{yt}, and the polynomial of $\tan\theta$ becomes

$$\left\{\frac{1+\frac{1}{n_{fc}\rho_{ft}}\left[1-\frac{e_h-n_{fc}\rho_{ft}\epsilon_{0t}+n_{sc}\rho_t(f_{yt}/E_s)}{n_{sc}\rho_t(f_{yt}/E_s)+n_{fc}\rho_{ft}\epsilon_t+e_h-n_{fc}\rho_{ft}\epsilon_{0t}}\right]}{1+\frac{1}{n_{fc}\rho_{fl}}}\right\}\tan^4\theta$$

$$+\left\{\frac{e_v-n_{fc}\rho_{fl}\epsilon_{0l}+n_{sc}\rho_l(f_{yl}/E_s)}{(1+n_{fc}\rho_{fl})[n_{sc}\rho_t(f_{yt}/E_s)+n_{fc}\rho_{ft}\epsilon_t+e_h-n_{fc}\rho_{ft}\epsilon_{0t}]}\right\}\tan^2\theta-1=0 \tag{11}$$

Step (d). Analysis after Yielding of Effective Vertical Reinforcement and before Yielding of Effective Horizontal Reinforcement

The analysis is carried out as in Step (a) above with $f_l=f_{yl}$. The shear stress ν is given by Eq. (8), and the polynomial of $\tan\theta$ becomes

$$\left\{\frac{1+\frac{1}{n_{sc}(\rho_t+n_{fs}\rho_{ft})}\left[1-\frac{e_h-n_{fc}\rho_{ft}\epsilon_{0t}}{n_{sc}(\rho_t+n_{fs}\rho_{ft})\epsilon_l+e_h-n_{fc}\rho_{ft}\epsilon_{0t}}\right]}{1+\frac{1}{n_{fc}\rho_{fl}}}\right\}\tan^4\theta$$

$$+\left\{\frac{e_v-n_{fc}\rho_{fl}\epsilon_{0l}+n_{sc}\rho_l(f_{yl}/E_s)}{(1+n_{fc}\rho_{fl})[n_{sc}(\rho_t+n_{fs}\rho_{ft})\epsilon_t+e_h-n_{fc}\rho_{ft}\epsilon_{0t}]}\right\}\tan^2\theta-1=0 \tag{12}$$

Step (e). Compressive Crushing of Concrete

During any of the preceding states the concrete may crush; this will define failure of the joint. Crushing will occur when the principal compressive stress, σ_2, reaches the strength of concrete, $f_c^{\max}$. The stress-strain relationship assumed here along the principal compressive direction is that described in Pantazopoulou and Bonacci (1992):

$$\sigma_2=f_c^{\max}\left[2\frac{\epsilon_2}{\epsilon_{\max}}-\left(\frac{\epsilon_2}{\epsilon_{\max}}\right)^2\right] \quad \text{where} \quad \left\{\begin{array}{c} f_c^{\max}=\lambda f_c \\ \epsilon_{\max}=\lambda\epsilon_0 \\ \lambda=\dfrac{1+\rho_{sv}|f_{ys}/f_c|}{0.8-0.34(\epsilon_1/\epsilon_0)} \end{array}\right\} \tag{13}$$

where f_c and $\epsilon_0(=-0.002)$ are the compressive strength and failure strain of concrete in uniaxial compression (they both carry negative signs) and ρ_{sv} is the volume ratio of stirrups.

Step (f). Failure of FRP

The FRP will fail by tensile fracture when the tensile stress (f_{ft} or f_{fl}) reaches the tensile strength, f_{fu}. Debonding is treated here according to the fractural mechanics-based model of Holzenkämpfer (1994). This model is slightly modified here to give the maximum tensile stress in an FRP strip of thickness t_f in millimeters (mm) when debonding occurs, equal to

$$f_{f,\text{deb}}=f_f^{\max}=c_1\sqrt{\frac{E_f f_{\text{ctm}}}{t_f}} \quad \text{for } \ell_b\geq\ell_{b,\max} \tag{14}$$

$$f_{f,\text{deb}}=f_f^{\max}\frac{\ell_b}{\ell_{b,\max}}\left(2-\frac{\ell_b}{\ell_{b,\max}}\right) \quad \text{for } \ell_b<\ell_{b,\max} \tag{15}$$

where f_{ctm} is the mean tensile strength of concrete in mega pascals (MPa), ℓ_b is the bond length (in mm), and

$$\ell_{b,\max}=\sqrt{\frac{E_f t_f}{c_2 f_{\text{ctm}}}} \tag{16}$$

Note that in Eqs. (14) and (16) E_f is given in mega pascals. Moreover, as equilibrium of the joint is studied at midwidth and midheight, ℓ_b is taken as approximately equal to the distance from the end of the FRP to the middle of the joint core (Fig. 1). Finally, Neubauer and Rostásy (1997) have shown that in the case of CFRP the constants c_1 and c_2 in Eqs. (14) and (16) take the values 0.64 and 2, respectively.

Solution Procedure

The analytical formulation given above was implemented in a computer program specifically developed for the analysis of RC joints strengthened with FRP strips. The user inputs a series of material and geometric characteristics, and the program traces the state of stress and strain in the joint until failure. Input to the program consists of (1) the geometric variables $\rho_s, \rho_b, \rho_{c,in}, \rho_c, \rho_{ft}, \rho_{fl}$; (2) the bond condition variables β_t and β_l; (3) the material properties f_c, f_{ctm}, and ϵ_0 for concrete, E_s,

f_{yl}, f_{ys}, and f_{yb} for steel, E_f, f_{fu}, and $f_{f,\text{deb}}$ for FRP; (4) the normalized axial forces N_v/bd and N_h/bh; and (5) the initial strain ϵ_{0t} in the joint (at the moment of strengthening).

As a first step, the program calculates the initial strain ϵ_{0l} required to satisfy equilibrium of the joint (without the FRP). Next, the strain ϵ_t is incremented, and for each value of ϵ_t Eq. (9) is solved for $\tan\theta$, so that the shear stress ν may be calculated [Eq. (8)]. The values of ν and $\tan\theta$ are then used to calculate all other stresses and strains [Eqs. (2)–(6)]. When first yielding of the reinforcement occurs (this is checked at each step by comparing steel strains to yield values), the analysis proceeds with mechanisms (or steps) (b) or (d) described above, either of which may be followed by mechanism (c). The value of $\tan\theta$ is always obtained by solving the equation corresponding to the mechanism that is active in each step. At the end of each step the program checks for two conditions: (1) concrete crushing [through Eq. (13)], which signals termination of the analysis and defines the shear capacity of the joint, $\nu_{\max}$; and (2) failure of the FRP [$f_{fl}=\min(f_{f,\text{deb}},f_{fu}), f_{ft}=\min(f_{f,\text{deb}},f_{fu})$], which again terminates the analysis and defines the shear capacity (at least equal to that of the joint as if no FRP had been applied, $\nu_{0,\max}$).

In principle, E_c is to be obtained through a secant modulus iteration scheme at each step. However, extensive analyses performed by the writers on FRP-strengthened joints as well as by Pantazopoulou and Bonacci (1992) on RC joints without FRP led to the conclusion that quite similar results can be obtained without iteration by choosing E_c to be the secant modulus at peak stress; this value may be assumed equal to $2f_c/\epsilon_0$, that is, $E_c=1{,}000f_c$.

Joints Strengthened with Flexible Sheets or Fabrics

The assumption of unidirectional strips bonded in the horizontal and vertical directions is relaxed in this section. The FRP material considered here consists of sheets or fabrics (with fibers in directions that do not coincide necessarily with the vertical and/or horizontal) that are stacked to form a laminate of thickness t_f. In this case, $\rho_{ft}=\rho_{fl}=\rho_f=nt_f/b$, where n is the number of laminates ($n=2$ for two-sided patching, when both sides of the joint are accessible; $n=1$ for one-sided patching, when a transverse beam exists so that application of the FRP on both sides is not possible).

Stresses and strains in the composite material are coupled according to the following constitutive law:

$$\begin{bmatrix} f_{ft} \\ f_{fl} \\ f_{\text{ftl}} \end{bmatrix} = \begin{bmatrix} Q_{11} & Q_{12} & Q_{13} \\ Q_{12} & Q_{22} & Q_{23} \\ Q_{13} & Q^{23} & Q_{33} \end{bmatrix} \cdot \left(\begin{bmatrix} \epsilon_l \\ \epsilon_l \\ \gamma \end{bmatrix} - \begin{bmatrix} \epsilon_{0t} \\ \epsilon_{0l} \\ \gamma_0 \end{bmatrix} \right) \tag{17}$$

where f_{ftl} is the shear stress in the composite material, γ is the shear strain in the joint, and Q_{ij} $(i,j=1,2,3)$ are elements of the composite material stiffness matrix that depend on the properties (four elastic constants and thickness) of the various laminae (layers) that have been stacked to form the joint's external reinforcement. Details about these elements may be found in standard texts on composite materials [e.g., Jones (1975)].

The shear strain γ in the joint equals

$$\gamma=\frac{2(\epsilon_l-\epsilon_t)}{\tan\theta}=\frac{-2\tan\theta(\epsilon_l-\epsilon_t)}{1-\tan^2\theta} \tag{18}$$

By introducing the above matrix formulation, the equilibrium relationships given by Eqs. (5)–(6) are written as follows:

$$\sigma_t=-\rho_t f_t-\rho_f[Q_{11}(\epsilon_t-\epsilon_{0t})+Q_{12}(\epsilon_l-\epsilon_{0l})+Q_{13}(\gamma-\gamma_0)]-\frac{N_h}{bh} \tag{19}$$

$$\sigma_l=-\rho_l f_l-\rho_f[Q_{12}(\epsilon_t-\epsilon_{0t})+Q_{22}(\epsilon_l-\epsilon_{0l})+Q_{23}(\gamma-\gamma_0)]-\frac{N_v}{bd} \tag{20}$$

Next we analyze the four basic states of joint behavior, as in the previous section.

Step (a). Analysis before Yielding of Steel Reinforcement

We start with Eq. (7) and write the stress σ_2 in terms of ν and $\tan\theta$, using Eqs. (2)–(4). The resulting expression is

$$-\nu n_{sc}\tan^3\theta-\epsilon_t E_s\tan^2\theta+\frac{n_{sc}\nu}{\tan\theta}+\epsilon_l E_s \tag{21}$$

Next we write Eq. (19) with σ_t replaced by $-\nu\tan\theta$, γ replaced by the right term in Eq. (18), and $f_t=E_s\epsilon_t$. The result is obtained in terms of ν as follows:

$$\nu=\frac{1}{\tan\theta}\left[\rho_t E_s\epsilon_t+\rho_f\left(Q_{11}+\frac{2Q_{13}\tan\theta}{1-\tan^2\theta}\right)\epsilon_t+\rho_f\left(Q_{12}-\frac{2Q_{13}\tan\theta}{1-\tan^2\theta}\right)\epsilon_l-\rho_f K_1+\frac{N_h}{bh}\right] \tag{22}$$

where

$$K_1=Q_{11}\epsilon_{0t}+Q_{12}\epsilon_{0l}+Q_{13}\gamma_0 \tag{23}$$

Finally, we write Eq. (20) with σ_l replaced by $-\nu/\tan\theta$, γ replaced by the right term in Eq. (18), $f_l=E_s\epsilon_l$, and ν as given in Eq. (22). The result in terms of ϵ_l is as follows:

$$\epsilon_l=\frac{(\rho_t E_s+\rho_f A)\epsilon_t-\rho_f(K_1-K_2\tan^2\theta)+\frac{N_h}{bh}-\frac{N_v}{bd}\tan^2\theta}{\rho_f B+\rho_l E_s\tan^2\theta} \tag{24}$$

where

$$A=\left(Q_{11}+\frac{2Q_{13}\tan\theta}{1-\tan^2\theta}\right)-\left(Q_{12}+\frac{2Q_{23}\tan\theta}{1-\tan^2\theta}\right)\tan^2\theta \tag{25}$$

$$B=-\left(Q_{12}-\frac{2Q_{13}\tan\theta}{1-\tan\theta}\right)+\left(Q_{22}-\frac{2Q_{23}\tan\theta}{1-\tan^2\theta}\right)\tan^2\theta \tag{26}$$

$$K_2=Q_{12}\epsilon_{0t}+Q_{22}\epsilon_{0l}+Q_{23}\gamma_0 \tag{27}$$

Step (b). Analysis after Yielding of Effective Horizontal Reinforcement and before Yielding of Effective Vertical Reinforcement

The analysis is carried out as in Step (a) above with $f_t=f_{yt}$. Hence ν is given by Eq. (22) with the product $E_s\epsilon_t$ replaced by f_{yt}, and the expression for ϵ_l becomes

$$\epsilon_l=\frac{\rho_f A\epsilon_t-\rho_f(K_1-K_2\tan^2\theta)+\frac{N_h}{bh}-\frac{N_v}{bd}\tan^2\theta+\rho_t f_{yt}}{\rho_f B+\rho_l E_s\tan^2\theta} \tag{28}$$

Analysis after Yielding of Both Horizontal and Vertical Reinforcement

The analysis is carried out as in Step (a) above with $f_t=f_{yt}$ and $f_l=f_{yl}$. Hence ν is given by Eq. (22) with the product $E_s\epsilon_t$ replaced by f_{yt}, and the expression for ϵ_l becomes

$$\epsilon_l = \frac{\rho_f A \epsilon_t - \rho_f (K_1 - K_2 \tan^2\theta) + \frac{N_h}{bh} - \frac{N_v}{bd}\tan\theta + \rho_t f_{yt} - \rho_t f_{yl}\tan^2\theta}{\rho_f B} \quad (29)$$

Analysis after Yielding of Effective Vertical Reinforcement and before Yielding of Effective Horizontal Reinforcement
Here too, the analysis is carried out as in Step (a) above with $f_l = f_{yl}$. The shear stress ν is given by Eq. (22), and ϵ_l is

$$\epsilon_l = \frac{(\rho_t E_s + \rho_f A)\epsilon - \rho_f (K_1 - K_2 \tan^2\theta) + \frac{N_h}{bh} - \frac{N_v}{bd}\tan^2\theta - \rho_l f_{yl}\tan^2\theta}{\rho_f B} \quad (30)$$

Solution Procedure

The analytical formulation given above was implemented in a computer program specifically developed for the analysis of RC joints strengthened with flexible sheets or fabrics. Regarding input to the program, the only difference from the previous section lies in the introduction of the FRP material properties: the user describes the geometric and elastic constants of the various laminae forming the FRP laminate, and the program calculates the elements Q_{ij} of the stiffness matrix. Moreover, the user defines the failure criterion for fracture of the laminate. For the most common case of laminates with fibers in the two orthogonal directions (l and t), it is sufficient to define the ultimate FRP stress, $f_{fu,t}$ in the direction t and $f_{fu,l}$ in the direction l. Upper limits to the FRP stress are also introduced to account for debonding; these values are estimated using the approach described in the previous section with E_f taken equal to Q_{11} or Q_{22}, for the limiting values of f_{ft} or f_{fl}, respectively.
The solution algorithm follows principles similar to those presented in the previous section: the strain ϵ_t is incremented, and through an iteration scheme Eqs. (21), (22), and (24) are solved for $\tan\theta$, ν, and ϵ_l. The value of ϵ_l is always obtained by solving the equation corresponding to the state that is active in each step. At the end of each step the program checks for FRP debonding or concrete crushing, which define the shear capacity $\nu_{\max}$.

Numerical Case Studies of FRP-Strengthened Joints

Case Study 1

In the preceding sections algebraic expressions were derived for stresses and strains in RC joints strengthened with FRP materials at various states of the steel reinforcement (elastic, postyield). In this section the equations for joint shear strength are applied to a generic joint strengthened with flexible sheets applied in several layers (laminae). The joint is assumed to be reinforced with a lot more reinforcement in the column than in the beam ($\rho_l = 0.015, \rho_t = 0.006$). Each FRP layer (lamina) consists of unidirectional carbon fibers in an epoxy matrix and has the following elastic constants: elastic modulus parallel to the fibers $E_{\parallel} = 180$ GPa, elastic modulus perpendicular to the fibers $E_{\perp} = 10$ GPa, shear modulus $G_{\parallel,\perp} = 5$ GPa and Poisson's ratio $\nu_{\parallel,\perp} = 0.25$.
If FRP debonding is prevented (e.g., through the use of mechanical anchors), absolute dimensions of the joint need not be specified, as they serve only to normalize steel/FRP quantities and axial loads. But if debonding dominates, we need to know t_f, that is, $b\rho_f/n$, and the FRP bond length in each direction. Hence, for each ρ_f we need to know the number of joint sides covered by the FRP ($n = 1$ or 2) and the width of the beam, b. In this case study $b = 250$ mm and $n = 2$. The bond lengths along the t and l directions are taken as $\ell_{bt} = 250$ mm and $\ell_{bl} = 500$ mm.
Next we define as V_l and V_t the volume fraction (within the laminate) of layers placed in the column and beam direction, respectively ($V_l + V_t = 1$). The following four configurations of the carbon sheets are assumed: (1) all layers with the fibers in the direction of the beam, $V_l/V_t = 0/1$; (2) the number of layers with fibers in the beam direction is the same as that in the column direction, $V_l/V_t = 0.5/0.5$; (3) the layers with fibers in the beam direction are two times more than those with fibers in the column direction, $V_l/V_t = 0.33/0.67$; and (4) all layers with the fibers in the direction of the column, $V_l/V_t = 1/0$. A summary of the design parameters for the case study is given in Tables 1 and 2. From the initial strain ϵ_{0t} before strengthening of the joints the other two elements of the initial strain matrix are calculated as follows: $\epsilon_{0l} = -6.97\times10^{-5}$ and $\gamma_0 = 1.95\times10^{-4}$ for case A (low axial force); $\epsilon_{0l} = -3.52\times10^{-4}$ and $\gamma_0 = 1.86\times10^{-4}$ for case B (high axial force).

Application of the procedure described above gives the shear strength of the joint in terms of the amount of FRP, as shown in Figs. 4(a,b) for $N_v/bd = 2.5$ MPa and in Figs. 4(c,d) for $N_v/bd = 10$ MPa, respectively. Figs. 4(a,c) apply if debonding is prevented, and Figs. 4(b,d) apply with debonding taken into account. Each figure also gives the state of reinforcement at failure: steel

Table 1. Summary of Design Parameters for Case Studies

Case	f_c (MPa)	f_{ctm} (MPa)	ρ_l (-)	ρ_t (-)	f_{yl} (MPa)	f_{yt} (MPa)	$\frac{N_h}{bh}$ (MPa)	$\frac{N_y}{bd}$ (MPa)	ε_{ot} (-)
1A	25	1.97	0.015	0.006	400	310	0	2.5	0.0002
1B	25	1.97	0.015	0.006	400	310	0	10	0.0002
2A	25	1.97	0	0	—	—	0	2.5	0
2B	25	1.97	0	0	—	—	0	10	0

Table 2. FRP Properties for Case Studies

V_l/V_t	Q_{11} (GPa)	Q_{12} (GPa)	Q_{13} (GPa)	Q_{22} (GPa)	Q_{23} (GPa)	Q_{33} (GPa)	$f_{fu,t}$ (MPa)	$f_{fu,l}$ (MPa)
0/1	180.63	2.51	0	10.03	0	5	1800	100
0.5/0.5	95.33	2.51	~0	95.33	~0	5	950	950
0.33/0.67	122.52	2.48	~0	66.23	~0	4.95	1,220	660
1/0	10.03	2.51	0	180.63	0	5	100	1,800

may have yielded and the FRP may debond or fracture, the latter being the case when the ultimate strain ε_{fu} is reached (as an example, ε_{fu} is taken here as equal to 0.01, a value that might be considered a typical design value for carbon fibers).

The general conclusion is that if debonding is not an issue, the effectiveness (increase in shear capacity v) of FRP is quite substantial and, for a given ρ_f, improves as more fibers are placed horizontally. This result is not surprising, as for this particular case study the joint steel reinforcement is much higher in the vertical direction than in the horizontal. If debonding is accounted for, the effectiveness of the FRP is relatively limited. Moreover, the favorable effect of high axial load becomes more pronounced as more fibers are placed horizontally. Finally, FRP fracture is possible at low ρ_f only and occurs in the horizontal (beam) direction. In fact, for very low ρ_f the FRP may fracture prematurely before the ultimate capacity of the joint is reached, implying that following FRP fracture the joint may carry additional load until it fails as if no external reinforcement were present (this is why in Fig. 4 for very low ρ_f some lines fall below that of the control specimen).

Case Study 2

Here we apply the analytical model, assuming a similar type of strengthening (flexible sheets with material properties as in case study (1) of a joint with $\rho_{c,in}=\rho_s=0$ and perfect bond conditions, that is, $\beta_t=\beta_l=0$. Further, it is assumed that debonding has not occurred at failure of the joint. As shown in Figs. 5 and 6, either concrete crushing or FRP fracture will determine the joint's shear capacity. In these two figures solid lines represent the response of joints as if FRP fracture were not a dominating failure mode. Cutoff lines (only active ones, that is, those falling below or in-

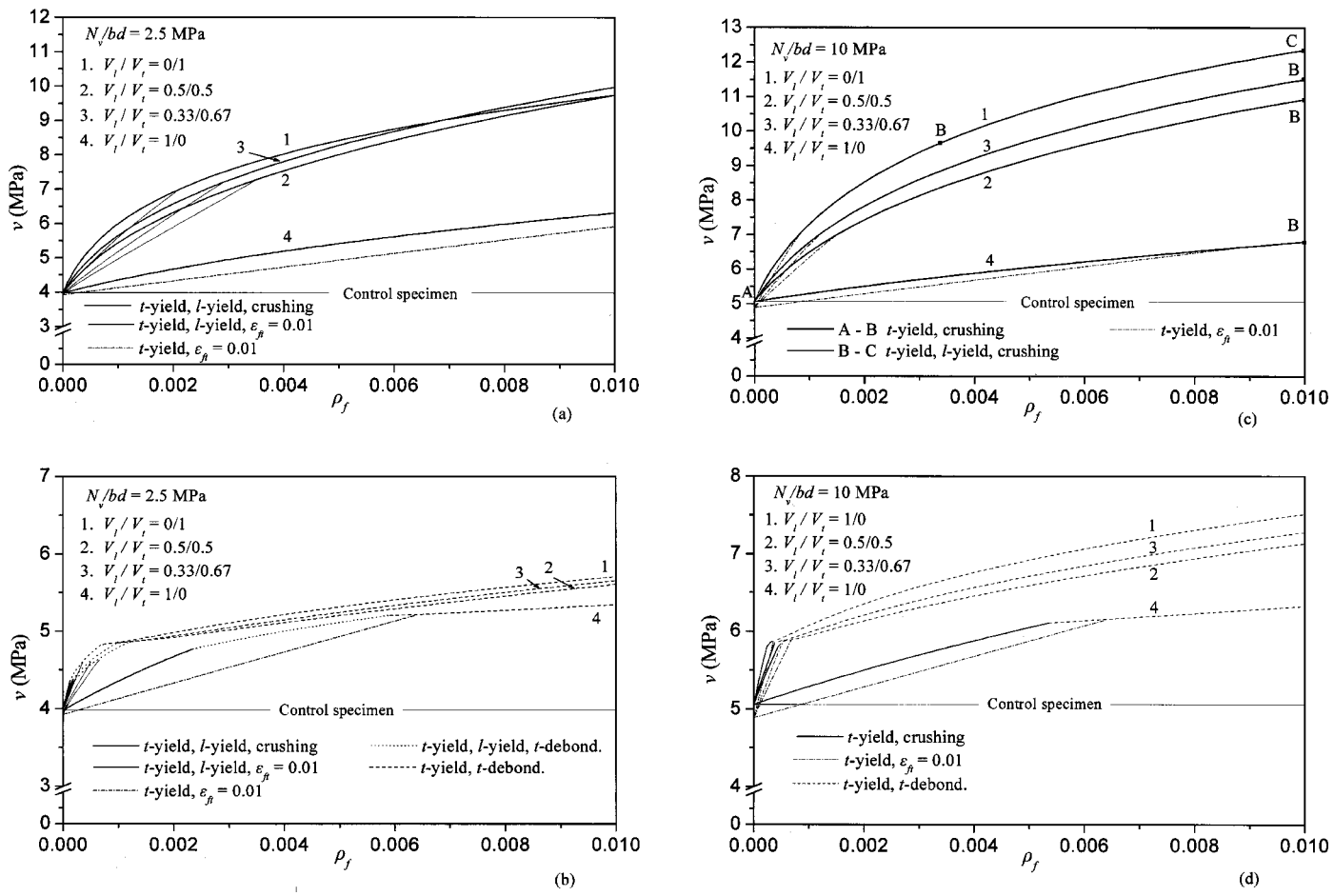

Fig. 4. Shear strength of FRP-strengthened joint in terms of ρ_f for various fiber distributions: (a) $N_v/bd=2.5$ MPa, no debonding; (b) $N_v/bd=2.5$ MPa, debonding is considered; (c) $N_v/bd=10$ MPa, no debonding; and (d) $N_v/bd=10$ MPa, debonding is considered (t-yield=yielding of beam reinforcement; l-yield=yielding of column reinforcement; t-debond=debonding of beam reinforcement).

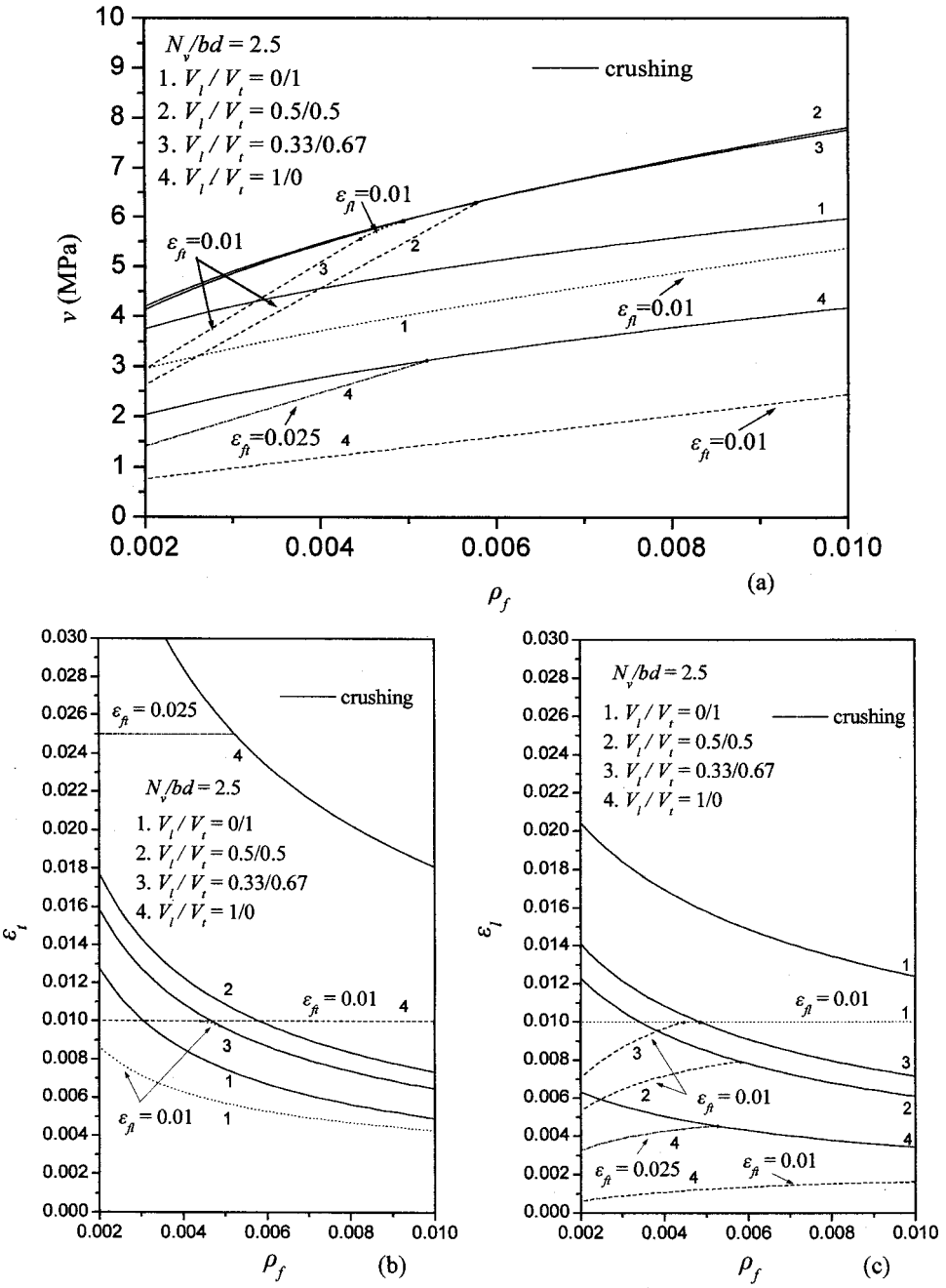

Fig. 5. Shear strength of FRP-strenghtened joint and FRP strains in terms of ρ_f for various fiber distributions and $N_v/bd = 2.5$ MPa: (a) shear strength; (b) FRP strain in beam direction; and (c) FRP strain in column direction.

tersecting the ones corresponding to concrete crushing) are provided for two different cases of FRP ultimate strain: 0.01 (e.g., typical design value for carbon fibers, dashed lines) and 0.025 (e.g., typical design value for glass or aramid fibers, dash-dot lines).

At relatively low axial loads in the column (Fig. 5), the increase in shear capacity is maximum when substantial percentages of fibers are placed both horizontally and vertically [cases 2 and 3 in Fig. 5(a)], and it is rather insensitive to the exact value of these percentages unless FRP fractures at low strains (0.01 assumed here); in the latter case placing more fibers in the beam rather than in the column gives the highest effectiveness. But as the axial load gets higher, placing the fibers in the horizontal direction gives the highest shear capacity [Fig. 6(a)].

Figs. 5(b,c) and 6(b,c) provide information about strains in the FRP. It is clear that at the joint's ultimate capacity the fibers are more effective (that is, they develop high strains) as ρ_f decreases; this is not the case if failure is dominated by FRP fracture.

Comparison of Analytical Model with Test Results

Experimental data on FRP-strengthened beam-column joints have been relatively limited. In order to validate the analytical model presented above and to obtain a more thorough understanding of the effect of various parameters on the behavior of RC joints; the writers conducted a comprehensive program that involved simulated seismic testing of approximately two-thirds scale T-joint

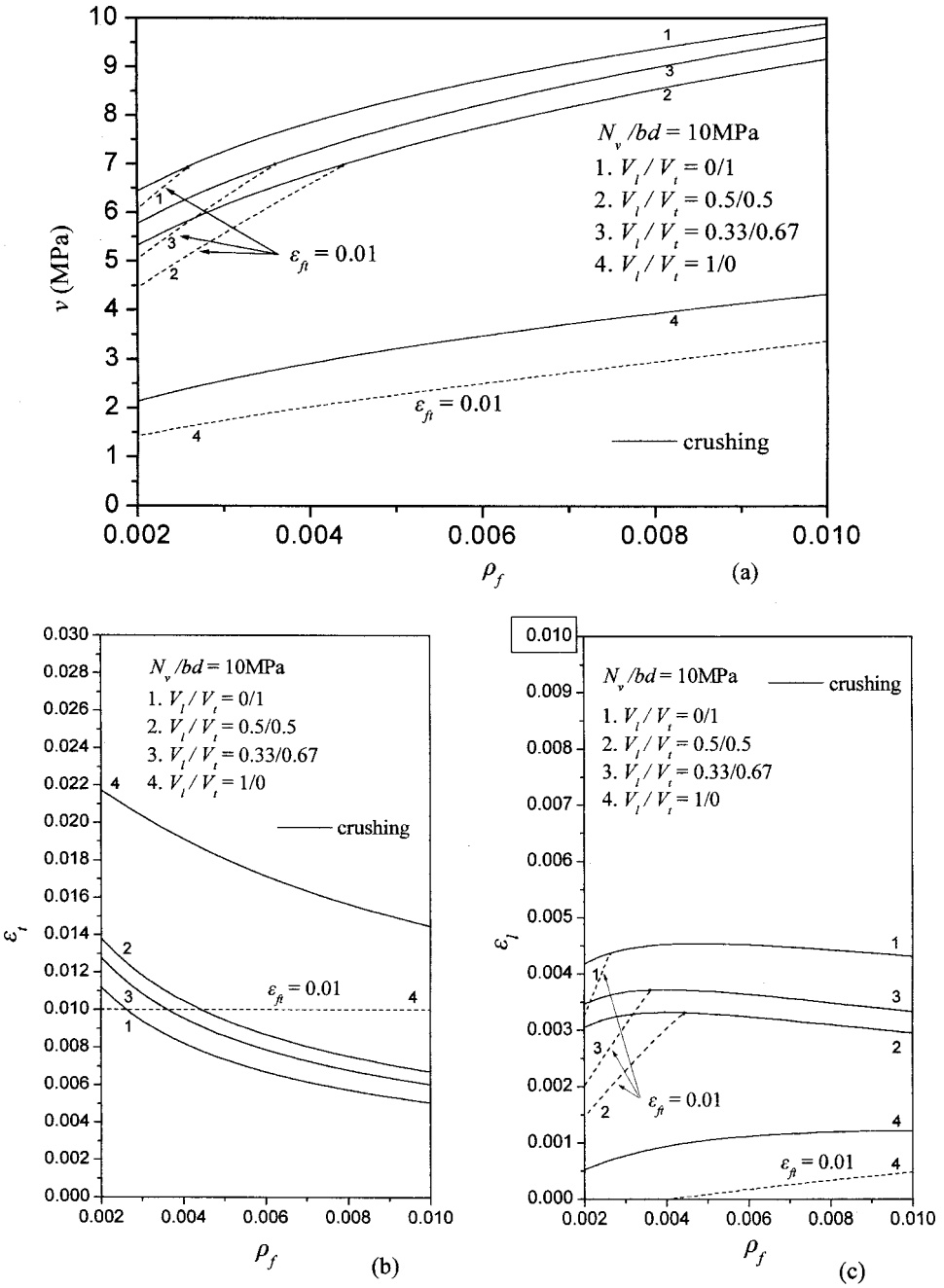

Fig. 6. Shear strength of FRP-strengthened joint and FRP strains in terms of ρ_f for various fiber distributions and $N_v/bd = 10$ MPa: (a) shear strength; (b) FRP strain in beam direction; and (c) FRP strain in column direction.

models. The joints were inadequately detailed (with no stirrups in the joint core), and the strengthening system was designed such that failure would occur due to shear. Earthquake loads were simulated by applying an alternating force (in a quasistatic cyclic pattern) to the end of the beam through an idealized pin, and the axial force in the column was kept constant. The displacement-controlled loading sequence for each specimen consisted of three cycles at a series of progressively increasing (by 5 mm) displacement amplitudes in each direction (push and pull) until a displacement of 45 mm was reached. Details about these tests may be found in the recent article of Antonopoulos and Triantafillou (2001). From the load versus displacement curves it was possible to record the peak force, corresponding to joint failure, and based on that to calculate (1) the tensile force T_b in the main beam reinforcement (calculated from cross-section analysis); and (2) the shear force V_c at the column face. The quantity $(T_b - V_c)/bd$ gives the experimentally obtained value for the shear strength of the joint, $v_{\max}$, which may be compared with the prediction of the analytical model.

Another set of (in principle) similar test results available in the literature is that of Gergely et al. (2000), who tested (differently detailed, compared to the above specimens) T-joints strengthened with CFRP and calculated the shear stress based on the experimentally measured load applied at failure of the joints.

Both sets of test data described above were used to evaluate the proposed analytical model. A few test results were omitted from the comparison because the associated strengthening designs were considered either unsuccessful or unrealistic: three joints in the

Table 3. Comparison of Analytical Model Predictions with Test Results

Specimen	f_c (MPa)	(MPa)	$(L/\theta)^{4d}$	$\frac{N_y}{bd}t_f$ (mm)	ρ_f ($\times 10^{-3}$)	$E_\parallel$ (GPa)	$\nu_{max}-$Exp (Mpa)	$\nu_{max}-$Anal (MPa)	$\frac{\nu_{max}-\text{Anal}}{\nu_{max}-\text{Exp}}$
AT(F11)	22.8	1.15	2/0°, 2/90°	0.13	2.6	230	4.64	4.50	0.97
AT(F22)	27.2	1.15	4/0°, 4/90°	0.13	5.2	230	5.37	6.62	1.23
AT(F21)	27.0	1.15	4/0°, 2/90°	0.13	3.9	230	5.47	5.75	1.05
AT(F12)	29.5	1.15	2/0°, 4/90°	0.13	3.9	230	4.74	5.84	1.23
AT(F22W)	29.2	1.15	4/0°, 4/90°	0.13	5.2	230	6.15	6.88	1.12
AT(GL)	19.5	1.15	5/0°, 5/90°	0.17	8.4	70	4.80	4.36	0.91
AT(SF22)[b]	19.0	1.15	4/0°, 4/90°	0.13	5.2	230	4.81	5.68	1.18
AT(T-F33)	26.0	1.15	3/0°, 3/90°	0.13	3.8	230	4.80	5.66	1.18
AT(T-F22S2)[c]	22.0	1.15	2/0°, 2/90°	0.13	2.6	230	4.33	4.42	1.02
GPR(4)	20.0	0	2/45°, 2/−45°	1.32	15.0	64.7	2.36	3.04	1.29
GPR(8)	20.0	0	2/45°, 2/−45°	1.32	15.0	64.7	2.36	3.04	1.29
GPR(9)	20.0	0	2/45°, 2/−45°	1.32	15.0	64.7	2.56	3.04	1.19
GPR(12)	34.0	0	2/45°, 2/−45°	1.32	15.0	64.7	2.59	3.04	1.17
GPR(13)	34.0	0	2/45°, 2/−45°	1.32	15.0	64.7	2.58	3.04	1.18
GPR(14)	34.0	0	2/45°, 2/−45°	1.32	15.0	64.7	2.96	3.04	1.02

Note: AT=Antonopoulos and Triantafillou (2001); GPR=Gergely et al. (2000).

[a]Notation in brackets denotes specimens as defined by those who conducted tests.

[b]$\rho_s=0.0017$; $\rho_{sv}=0.0034$; $f_y=265$ MPa.

[c]Strips placed on one side of joint debonded well before peak load (strength) was reached and were ignored.

[d]L denotes total number of layers on both sides of joint at angle θ from horizontal.

study by Antonopoulos and Triantafillou (2001) were strengthened with stiff strips that debonded quite early (before the peak load was reached), whereas four joints in the study by Gergely et al. (2000) were strengthened with unrealistically low quantities (resulting in extremely low axial rigidity) of FRP. The comparison between analytical and experimental values for the joint shear strength is given in Table 3, along with the design parameters for each test. Unless described differently in the table, in all these tests ρ_s and $\rho_{c,in}$ were equal to zero and the bond of rebars was assumed perfect, corresponding to $\beta_t=\beta_l=0$. The last assumption was verified in the tests of Antonopoulos and Triantafillou (2001), whereas no details are provided by Gergely et al. (2000) regarding rebar slip.

The writers found the agreement between analysis and test results surprisingly good and feel confident that the analytical procedure developed in this study may be used as a valuable tool toward the design of FRP externally bonded reinforcement for shear strengthening of beam-column joints.

Conclusions

Analytical models are presented in this study for the analysis of RC joints strengthened with composite materials in the form of externally bonded reinforcement comprising unidirectional strips or flexible fabrics. The models provide equations for stresses and strains at various stages of the response until the ultimate capacity is reached, defined by concrete crushing or FRP failure due to fracture or debonding. Solutions to these equations are obtained numerically.

The models provide useful information on the shear capacity of FRP-strengthened joints in terms of the quantity and configuration of the externally bonded reinforcement and may be used to design FRP reinforcement for inadequately detailed beam-column joints.

A few parametric analyses carried out in this study indicate that even low quantities of FRP materials may provide significant enhancement of the shear capacity. The effectiveness of external reinforcement increases considerably if debonding is suppressed (e.g., through proper anchorage) and depends heavily on the distribution of layers in the beam and the column. The latter depends on the relative quantities of steel reinforcement crossing the joint panel and the level of axial load in the column.

Shear-strength predictions provided by the analytical models were found in extremely good agreement with 15 experimental results found in the literature, thus adding confidence to the validity of the proposed equations.

Acknowledgments

Partial support to this research has been provided by the Research Committee of the University of Patras (''K. Karatheodoris'' Program) and by the General Secretariat for Research and Technology (PENED 1999).

Notation

The following symbols are used in this paper:

- b = width of beam;
- d = width of column;
- E_c = secant elastic modulus of concrete;
- E_f = elastic modulus of FRP strips in principal fiber direction;
- E_s = elastic modulus of steel;
- $E_\parallel$ = elastic modulus of single FRP layer parallel to fibers;
- $E_\perp$ = elastic modulus of single FRP layer perpendicular to fibers;

f_{by} = yield stress of beam reinforcement;
f_{cy} = yield stress of column reinforcement;
f_c = strength of concrete in uniaxial compression;
$f_c^{\max}$ = strength of concrete;
f_{ctm} = mean tensile strength of concrete;
$f_{f,deb}$ = stress in FRP when debonding occurs;
f_{fl} = average normal stress in FRP along direction l (at midheight of joint);
f_{ft} = average normal stress in FRP along direction t (at midwidth of joint);
f_{ftl} = shear stress in FRP laminate;
f_{fu} = tensile strength of FRP strip;
$f_{fu,l}$ = tensile strength of FRP laminate along direction l;
$f_{fu,t}$ = tensile strength of FRP laminate along direction t;
f_{sy} = yield stress of stirrups,
f_t = average stress in horizontal stirrups (at midwidth of joint);
f_{yt} = effective yield stress of horizontal reinforcement;
$G_{\parallel,\perp}$ = shear modulus of single FRP layer;
h = height of beam;
l = longitudinal (column) direction;
ℓ_b = FRP bond length;
ℓ_{bl} = FRP bond length along direction l;
ℓ_{bt} = FRP bond length along direction t;
N_h = compressive axial load in beam;
N_v = compressive axial load in column;
n = number of joint sides covered by FRP;
Q_{ij} = ij element of FRP laminate stiffness matrix;
T_b = tensile force in main beam reinforcement;
t = transverse (beam) direction;
t_f = thickness of FRP;
V_c = shear force at column face;
V_l = percentage of layers placed along direction l;
V_t = percentage of layers placed along direction t;
β_l = ratio of average stress in column reinforcement outside core to average stress of column reinforcement inside core at beam centerline;
β_t = ratio of average main beam reinforcement stress to average stirrup stress at column centerline;
γ = average shear strain of joint panel;
γ_0 = average shear strain of joint at moment of strengthening;
ε_{fu} = ultimate FRP strain;
ε_l = average normal strain along direction l of joint panel;
ε_{l0} = normal strain along direction l of joint at moment of strengthening;
ε_t = average normal strain along direction t of joint panel;
ε_{t0} = normal strain along direction t of joint at moment of strengthening;
ε_0 = failure strain of concrete in uniaxial compression;
ε_1 = maximum principal strain;
ε_2 = minimum principal strain;
θ = inclination (from t axis) of maximum principal strain ε_1;
ν = average joint shear stress;
$\nu_{\max}$ = joint shear strength;
$\nu_{0,\max}$ = shear strength of joint without FRP;
$\nu_{\parallel,\perp}$ = Poisson's ratio of single FRP layer;
ρ_b = total main beam reinforcement ratio;
ρ_c = total main column reinforcement ratio (at boundaries of joint core);
$\rho_{c,in}$ = column reinforcement ratio inside joint core;
ρ_{fl} = FRP reinforcement ratio along direction l;
ρ_{ft} = FRP reinforcement ratio along direction t;
ρ_l = effective vertical reinforcement ratio;
ρ_s = stirrup reinforcement ratio;
ρ_{sv} = volume ratio of stirrups;
ρ_t = effective horizontal reinforcement ratio;
σ_l = average stress in concrete along direction l;
σ_t = average stress in concrete along direction t;
σ_1 = maximum principal stress in concrete; and
σ_2 = minimum principal stress in concrete.

References

Alcocer, S., and Jirsa, J. O. (1993). "Strength of reinforced concrete frame connections rehabilitated by jacketing." *ACI Struct. J.*, 90(3), 249–261.

Antonopoulos, C. P., and Triantafillou, T. C. (2001). "Experimental investigation of FRP-strengthened RC beam-column joints." J. Compos. Constr., accepted.

Beres, A., El-Borgi, S., White, R. N., and Gergely, P. (1992). "Experimental results of repaired and retrofitted beam-column joint tests in lightly reinforced concrete frame buildings." *Technical Report NCEER-92-0025*, State Univ. of New York at Buffalo.

Gergely, I., Pantelides, C. P., Nuismer, R. J., and Reaveley, L. D. (1998). "Bridge pier retrofit using fiber-reinforced plastic composites." *J. Compos. Constr.*, 2(4), 165–174.

Gergely, J., Pantelides, C. P., and Reaveley, L. D. (2000). "Shear strengthening of RC T-joints using CFRP composites." *J. Compos. Constr.*, 4(2), 56–64.

Ghobarah, A., Aziz, T. S., and Biddah, A. (1997). "Rehabilitation of reinforced concrete frame connections using corrugated steel jacketing." *ACI Struct. J.*, 4(3), 283–294.

Holzenkämpfer, P. (1994). "*Ingenieurmodelle des verbundes geklebter Bewehrung für Betonbauteile*." PhD dissertation, TU Braunschweig, Germany.

Jones, R. M. (1975). *Mechanics of composite materials*. Scripta Book Company, Washington, D.C.

Neubauer, U., and Rostásy, F. S. (1997). "Design aspects of concrete structures strengthened with externally bonded CFRP-plates." *Concrete+Composites, Proceedings of the 7th International Conference on Structural Faults and Repair*, Vol. 2, 109–118.

Pantazopoulou, S., and Bonacci, J. (1992). "Consideration of questions about beam-column joints." *ACI Struct. J.*, 89(1), 27–36.

Pantelides, C. P., Gergely, I., Reaveley, L. D., and Nuismer, R. J. (1997). "Rehabilitation of cap beam-column joints with carbon fiber jackets." *Proc., 3rd Int. Symp. on Non-Metallic (FRP) Reinforcement for Concrete Structures*, Japan Concrete Institute, Sapporo, Japan, Vol. 1, 587–595.

Pantelides, C. P., Gergely, J., Reaveley, L. D., and Volnyy, V. (1999). "Retrofit of RC bridge pier with CFRP advanced composites." *J. Struct. Eng.*, 125(10), 1094–1099.

Paulay, T., and Priestley, M. J. N. (1992). *Seismic design of reinforced concrete and masonry buildings*," Wiley, New York.

Triantafillou, T. C., and Antonopoulos, C. P. (2000). "Design of concrete flexural members strengthened in shear with FRP." *J. Compos. Constr.*, 4(4), 198–205.

Tsonos, A. D., and Stylianidis, K. A. (1999). "Pre-seismic and post-seismic strengthening of reinforced concrete structural subassemblages using composite materials (FRP)." *Proc., 13th Hellenic Concrete Conference*, Rethymno, Greece, Vol. 1, 455–466 (in Greek).